ISSN 1063-7729, Astronomy Reports, 2016, Vol. 60, No. 10, pp. 894–903. © Pleiades Publishing, Ltd., 2016.
Original Russian Text © M.A. Il'ina, O.K. Sil'chenko, 2016, published in Astronomicheskii Zhurnal, 2016, Vol. 93, No. 10, pp. 860–870.

Analysis of the Structure of Disk Galaxies in the NGC 2300 Group

M. A. Il'ina[1] and O. K. Sil'chenko[1*]

[1] *Sternberg Astronomical Institute, Lomonosov Moscow State University, Universitetskii pr. 13, Moscow, Russia*

Received January 19, 2016; in final form, March 29, 2016

Abstract—Data from the 6-m telescope of the Special Astrophysical Observatory obtained using the SCORPIO instrument in imaging mode are used to study member galaxies of the NGC 2300 group. Surface photometry has been carried out for the five largest galaxies in the group, whose isophotal parameters and the parameters of their large-scale structural components (disks and bulges) have been determined. The morphological type of the central galaxy in the group has been refined, and shown to be elliptical. Studies of structural features in non-central disk galaxies have revealed an enhanced percent of bars: bars were found in all disk galaxies of this group, with all of these being compact structures. The similarity of the structural features of the disks of the group galaxies suggests that these disks may be being restructured in the process of the current merger of the two X-ray subgroups comprising NGC 2300: the group NGC 2300 itself and the group NGC 2276.

DOI: 10.1134/S1063772916100036

1. INTRODUCTION

According to [1], the vast majority of galaxies in the nearby Universe belong to groups with 2–100 members; thus, it is typical for these galaxies to evolve in a group environment. The characteristics of galaxy groups are quite varied, and they display a wide range of masses, velocity dispersions, and morphological types for the group members. When ROSAT data began to be used to carry out directed searches for hot intergalactic gas in groups, which should strongly influence their evolution and structure, and for star formation in disk galaxies, it turned out that diffuse X-ray emission was detected in only 30–50% of groups [2, 3]. We attempted in a series of studies to compare the evolution of galaxies in groups immersed in a hot, intergalactic media and those without a hot, intergalactic medium. Based on very small samples (two and three groups, respectively), we found hints that galaxies in groups that are *not* immersed in X-ray gas evolve synchronously, while the presence of hot gas gives rise to asynchronous outbursts of star formation [4]. However, due to the small size of the samples, this question remained open, and continues to be of interest.

In this study, which is a first paper dedicated to the nearby galaxy group NGC 2300, we present the results of surface photometry of a number of bright member galaxies. These photometric data were obtained on the 6-m telescope of the Special Astrophysical Observatory (SAO) of the Russian Academy of Sciences. The group NGC 2300 is well known and has been studied for a long time, since it is nearby and conveniently located in the northern sky. It was cataloged by Huchra and Geller [5], but only three galaxies had been identified as members at that time. Later, Garcia [6] composed a list of 13 members of the NGC 2300 group with magnitudes down to $B_0 = 14.0$ (for a distance to the group of 30.3 Mpc, according to EDD [7], this places a lower limit on the luminosity of $M_B = -18.4$), with 11 of these 13 members being spiral and irregular. In a recent revision of the list of nearby groups [1], the NGC 2300 group is divided into two: 11 galaxies belong to NGC 2300 subgroup and two to NGC 2276 subgroup, with this division being based on radial velocity, not position in the sky. It is curious that half of the total list of 13 galaxies (6 objects) diverges with the list of Garcia [6], but the morphological compositions of both groups are represented mainly by late-type galaxies. The only clearly lenticular galaxies in the NGC 2300/NGC 2276 group are NGC 2300 itself and IC 455, and no elliptical galaxies were reported in the group. A list of the bright galaxies considered in the current study, with characteristics collected from the literature, is presented in Table 1.

The origin of this morphological composition is not very clear, given that an appreciable intergalactic hot medium is present in the group. NGC 2300 was the first and a typical example of a relatively poor group of galaxies that displayed an X-ray signal indicating a diffuse, hot medium in the ROSAT

*E-mail: olga@sai.msu.su

Table 1. Global parameters of the studied galaxies

Galaxy	NGC 2300	IC 455	IC 469	IC 499	UGC 3654
Morphological type (NED,[1] LEDA[2])	SA0^0	S0	SAB(rs)ab	Sa	compact, S0
R''_{25}, (RC3,[3] LEDA)	85	33	66	63	32
B^0_T (RC3, LEDA)	11.77	14.01	12.87	12.91	14.61
M_B (RC3 + EDD[4])	−20.6	−18.4	−19.5	−19.5	−17.8
$(B-V)_T$ (RC3)	1.08	–	–	–	–
V_r, km/s (NED)	1905	2050	2080	1882	2303
Distance from center of group,[1] kpc	0	95	383	716	144
Distance to group,[5] Mpc	30.3				

[1] NASA/IPAC Extragalactic Database, http://ned.ipac.caltech.edu.
[2] Lyon-Meudon Extragalactic Database, HYPERLEDA, http://leda.univ-lyon1.fr.
[3] Third Reference Catalogue of Bright Galaxies [8].
[4] The Extragalactic Distance Database, http://edd.ifa.hawaii.edu.
[5] Cosmicflow-1 [7].

data [9]. It is interesting that the center of the X-ray emission did not coincide with NGC 2300 [9]—it was located in the space between NGC 2300 and NGC 2276. Both galaxies have the same blue luminosity but appreciably different 2 μm luminosities [1], and their radial velocities differ by 500 km/s. Since the morphology of NGC 2276 in the optical [10] and radio [11] has a clear cometary character, this galaxy is probably moving rapidly relative to the hot gas in the group, which compresses one side of the disk due to the ram pressure. In this case, NGC 2300 can undoubtedly be considered the central galaxy of the group, despite the fact that it is shifted relative to the center of the hot-gas distribution. Although the hot gaseous component of the NGC 2300 group is very extended—Mulchaey et al. [9] detected it at least 300 kpc from the center—the galaxies of the group are distributed over an even larger area, and many are located outside the X-ray spot (Table 1). It would be interesting to search for differences in the structure and evolution of the central and peripheral galaxies in the group.

2. OBSERVATIONS AND DATA ANALYSIS

The photometric data analyzed here were obtained at the prime focus of the SAO 6-m telescope using the SCORPIO instrument [12] operating in a direct-imaging regime. The receiver was an EEV 42-40 CCD array with 2048 × 2048 pixels 13.5 μm in size. The readout was carried out in a double-pixel regime providing a scale of 0.35″ per image element. The total field of view of the instrument was 6.1′ × 6.1′. The observations were conducted in two photometric bands with the standard Johnson B and V filters. Twilight was used as a flat field.

A detailed journal of observations is presented in Table 2, which gives the total exposure in each filter for each galaxy, the full width at half maximum (FWHM) of a stellar image in the frame (the so-called "seeing", which determines the spatial resolution of the data), and PA (top), which is the orientation on the sky of the upper edge of the CCD frame on the sky, where the position angle is measured counterclockwise from north. All the CCD frames for the galaxies in the NGC 2300 group were obtained on the night of September 2–3, 2008 under photometric conditons with seeing better than 2″. Five fields centered on the bright galaxies in the group were taken: NGC 2300, IC 455, IC 469, IC 499, and UGC 3654. In the reduction of the exposures, we corrected for the dark current, divided by a flat field, and subtracted the sky background. We determined the orientation and scale for each field by loading the corresponding FITS image to the site http://nova.astrometry.net.

Table 2. Photometric observations of the galaxies in the group NGC 2300

Galaxy	Filter	Total exposure, s	Seeing, $''$	PA (top)
NGC 2300	B	180	1.6	−0.4
NGC 2300	V	60	1.4	−0.4
IC 455	B	540	1.3	−3.6
IC 455	V	180	1.3	−3.6
IC 469	B	540	1.4	−2.8
IC 469	V	180	1.4	−2.8
IC 499	B	360	1.4	+5.0
IC 499	V	180	1.2	+5.0
UGC 3654	B	360	1.2	−3.9
UGC 3654	V	120	1.1	−3.9

We used the central galaxy of the group, NGC 2300, as a photometric standard for the magnitude calibration: the HYPERLEDA database contains a selection of aperture photometry data in the standard Johnson system for this galaxy. We tried to carry out the calibration using two datasets in the B and V filters based on CCD photometry from the surveys [13, 14], which were recalculated in the HYPERLEDA database to apertures with radii from $4''$ to $58''$. Both sets of aperture data gave similar zero points for the recalibration of the signal in magnitudes; however, the data of [14] showed a trend for the zero point with increasing aperture, which was especially noticeable in the B filter. As a result, we used a set of 39 aperture estimates based on the data of [13] for the calibration, and obtained the following constants to translate the signals into magnitudes: 31.12^m (B) and 29.84^m (V), with accuracy to better than 0.01^m, without any trend with aperture radius.

3. ISOPHOTAL ANALYSIS OF THE CENTRAL GALAXIES OF THE FIELDS

We determined the shapes and orientations of the galactic isophotes using the FITELL program developed by V.V. Vlasyuk [15]. Figure 1 presents the results of our isophote analysis for the five galaxies in the V filter. We comment on the results for each galaxy below.

IC 455. Judging from the dependences of the position angle and ellipticity on the distance from the center, this is not a homologous disk galaxy: a wave in the variations of the isophote major-axis position angle is observed over the entire interval of distances from the center, and the ellipticity reaches a maximum at $R \approx 15''-20''$, then slowly falls off.

UGC 3654. This shows a similar radial dependence for the ellipticity: a maximum is observed at $R \approx 15''-22''$, with the ellipticity first monotonically growing and then falling off before and after this value. The dependence of the position angle on distance from the center of the galaxy shows the presence of two local maxima—one near the center and the other near the maximum ellipticity—suggesting that the galaxy has a fairly large bar, and possibly a tri-axial bulge.

IC 469. The ellipticity emerges onto a plateau, $1 - b/a \approx 0.65$, at a distance $R \approx 30''$ from the center. It is probably from this radius that the large-scale disk begins to dominate the surface brightness. However, there is also a small local maximum in the ellipticity in the inner region, at $R \leq 10''$, and the isophote major axis turns sharply by 40° at this radius. It is likely that the galaxy possesses a bar that is small but displays a high contrast, although the SAB classification would not usually suggest the presence of a "strong" bar.

IC 499. The profile of the isophote ellipticity is very regular, although with some hint of a two-tiered disk structure with different thickness for the segments, with the boundary between the segments located at $R \approx 50''$. However, the orientation of the isophote major axis varies strongly in the central region of the galaxy, $R < 16''$. This suggests the value of searching for a bar in this galaxy.

NGC 2300. A hump at $R \approx 9''$ is observed in the radial dependence of the ellipticity, $1 - b/a = 0.23$, with this parameter showing a roughly constant value of about 0.17 at greater distances, suggesting the presence of a nested structure, whose nature can be determined only through further kinematic studies. It is also interesting that a minimum in the position angle with the value 74° is reached about $10''$ from the center of the galaxy, after which the isophote major axis turns to $PA \approx 90°$ by $R \approx 40''$. In outer regions, where $R > 70''$, this position angle returns to the value $PA \approx 74°$. The same behavior for the ellipticity and position angle can be seen in the analysis of 2 μm images of this galaxy in [16]. Although the galaxy is classified as not having a bar, the shape of the isophotes is not characteristic for an inner flat disk.

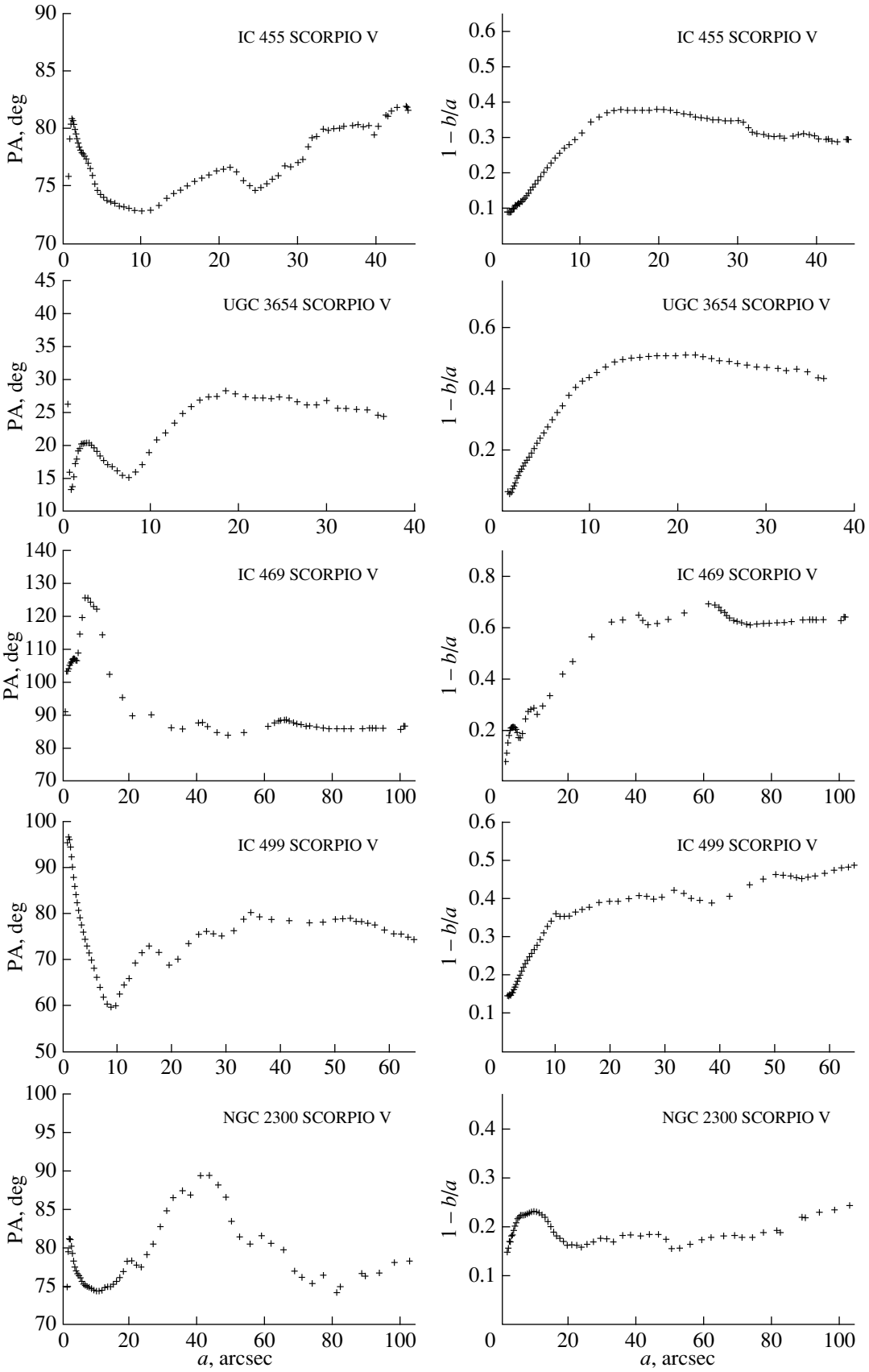

Fig. 1. Results of our isophotal analysis for the images of the studied galaxies in the V filter. Variations of the position angle of the isophote major axis (left) and ellipticity (right) with radius are shown.

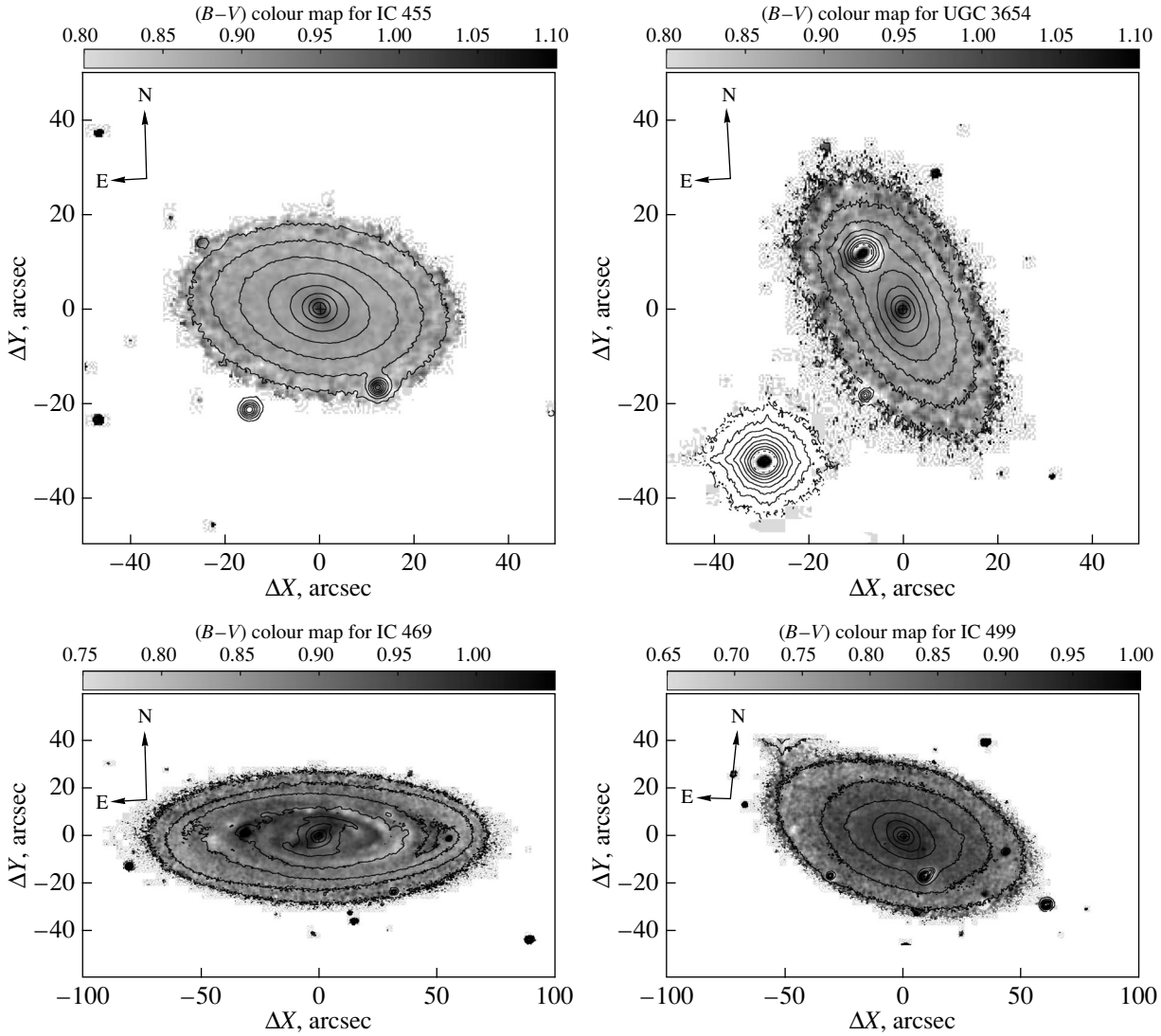

Fig. 2. $B-V$ map for four large galaxies in the NGC 2300 group. On top of the color map given by gray gradations, the V isophots are superimposed.

4. ANALYSIS OF STRUCTURE OF GALAXIES IN THE NGC 2300 GROUP

We constructed $B-V$ maps for the studied galaxies (Fig. 2), then calculated surface-brightness profiles (Fig. 3). Beginning from the center, we used FITELL (an azimuthal Fourier expansion) for this; in outer regions, we determined the major-axis positon angle and isophote ellipticity using the outermost points for which the isophote analysis was carried out, and, further from the center, we performed a simple average of the brightness along ellipses with specified shapes and various radii. We carried out a decomposition for the azimuthally averaged brightness profiles, distinguishing an exponential disk, sometimes with different scales in different radius intervals, and a Sersic bulge. We also searched for evidence of the presence of rings and bars.

A Sersic law [17] can be written

$$\mu(r) = \mu_e + 1.086 b_n[(r/r_e)^{1/n} - 1],$$

where n, r_e, and μ_e are parameters of the model and $b_n \approx 2n - 0.32$. Various special cases are known: $n = 1$ is an exponential profile, which is characteristic for large-scale stellar disks, and $n = 4$ is a de Vaucouleur law, which is more often encountered in massive elliptical galaxies and especially large bulges of disk galaxies. We distinguished the structural components of the galaxies beginning from outer regions, which we initially supposed to be disks with exponential brightness profiles [18]. After fitting the outer stellar disk using an exponential brightness profile and determining its parameters, we then constructed a two-dimensional model image and subtracted it from the observed galaxy image, after which the pro-

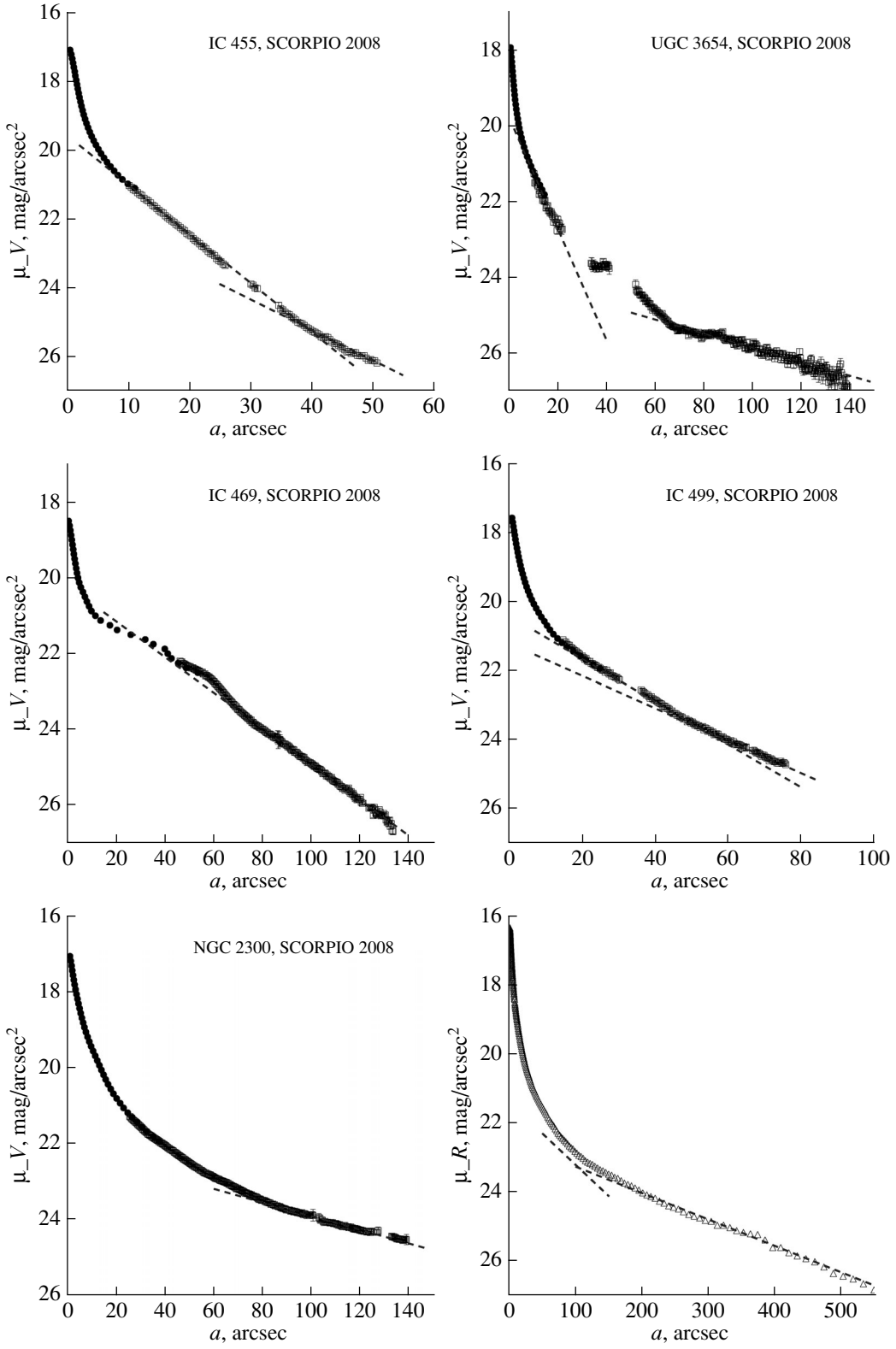

Fig. 3. *V* surface-brightness profiles for disk galaxies in the NGC 2300 group. The points show azimuthally averaged profiles for the central regions, with freely varying orientations and axial ratios for the ellipses along which the averaging was carried out, derived from the isophotal analysis carried out using the FITELL program. The shape of the ellipses in more outer regions was specified using the outer data from the isophotal analysis shown in Fig. 1; further, averaging was done using a fixed isophote geometry (shown by the squares). The dashed straight lines show exponential laws for the disk segments fitted to the profile (see the text). *R*-band data for NGC 2300 from [19] are shown in the bottom right panel, where a fit from [19] is shown in the outer part of the profile and our fit from the left panel is shown for the inner part.

Table 3. Parameters of photometric components of galaxies in the NGC 2300 group in the V filter

Name	Outer disk				Inner disk				Bulge			
	ΔR, $''$	μ_0, mag/□$''$	r_0, $''$	r_0, kpc	ΔR, $''$	μ_0, mag/□$''$	r_0, $''$	r_0, kpc	n	μ_e, mag/□$''$	r_e, $''$	r_e, kpc
U3654	70–130	24.0	58.4	8.6	7–35	19.8	7.4	1.1	2.6 ± 0.4	19.7	2.0	0.3
IC455	40–51	21.8:	12.35	1.8	10–40	19.6	7.65	1.1	2.5 ± 0.4	18.8	1.8	0.3
IC469	70–120	20.2	23	3.4	–	–	–	–	–	–	–	–
IC499	20–55	20.4	17.4	2.6	7–15	18.1	3	0.5	2.2 ± 0.4	19.7	4.8	0.7

cedure of constructing and fitting the azimuthally averaged surface-brightness profile was repeated. If the isophote ellipticity of the residual profile did not differ strongly from the ellipticity of the outer isophotes, we inferred the presence of a separate inner stellar disk, and fitting it separately with an exponential profile. After subtracting this inner disk, this left the central bulge, for which the Sersic parameter n was not fixed, and was varied.

Table 3 presents the parameters of our photometric models of the galaxies; the characteristic accuracy of the central surface brightnesses is 0.1^m per square arcsec, and the exponential scales were determined with accuracies no worse than $0.5''$. Both of the non-central lenticular galaxies proved to have two-tiered exponential disks and classical bulges, while the spiral galaxies at the periphery of the group can be described with a single exponential scale. All the galaxies were found to possess central bars, although none of them were initially classified as SB galaxies. In the process of constructing the model galaxy images and subtracting them from the observed images, we were able to distinguish small-scale peculiar structures in a number of cases in addition to the large-scale structural components, which are clearly visible in the color maps. We briefly describe the general structure and substructures of each galaxy below.

IC 455. The outer disk, $R > 40''$, is very weak, and its parameters are determined only uncertainly; it is possible that $\mu_{V,0} \approx 21.8$ and $r_0 \approx 12.4''$ over one exponential scale. The main stellar disk in the surface-brightness profile (Fig. 3) is distinguished by a long exponential segment with an extent of about four scale lengths: $\mu_{V,0} = 19.6$ and $r_0 = 7.6''$ in the range $R = 10''$–$40''$. After subtracting the model for this disk, two thick spiral, weakly wound arms become visible, which was not expected for the classification of this galaxy, S0. The isophotes of the residual emission display a different major-axis position angle, $PA \approx 50°$. Judging from the sharp growth in the isophote ellipticity as a function of radius, the residual emission may represent a bulge with segments emerging from the ends of a bar, at radii $R > 8''$. The brightness profile of the residual emission obeys a Sersic law. A very red substructure elongated in $PA \approx 45°$ (Fig. 2) also suggests the presence of a compact bar; spectral observations (described in a future paper) testify to a complete absence of gas, and consequently of dust, in the galaxy.

UGC 3654. According to the classification given in HYPERLEDA, this is either a compact S0 or a compact E galaxy. However, it is no smaller than IC 455 in size, and its morphology is also similar to that of IC 455. Attempts to fit the surface-brightness profile obtained in a circular aperture using a classical de Vaucouleur law (which would have suggested the galaxy was a classical elliptical) were unsuccessful. Therefore, we suggest that this galaxy is better classified as lenticular.

In this case, the outer disk of the galaxy begins from $70''$ (Fig. 3), and its surface brightness and radial scale are $\mu_{V,0} = 24.0$ and $r_0 = 58''$. The suggestion that the galaxy is lenticular is apparently true: after subtracting the outer disk, the residual emission is fit excellently by an exponential disk at $7''$–$35''$ from the center, with a surface brightness and radial scale of $\mu_{V,0} = 19.8$ and $r_0 = 7.4''$. It was logical to construct the brightness profile of the residual emission after subtracting the two model disks in a circular aperture, in order to search for the presence of a bulge component in the galaxy. The resulting brightness profile obeys a Sersic law at $R \leq 6''$. After subtracting this model bulge, a structure that may be a bar with weak spiral arms remains. The color map in the central region of the galaxy is asymmetric, and displays a red excess on the southeast side of the nucleus; this may be a dust ring around the bar.

IC 469. The observed surface-brightness profile can be firmly classified as a Freeman Type 2 profile [18]. We fitted the outer parts of the surface-brightness profile at radial distances of $70''-120''$ using a model exponential disk with $\mu_{V,0} = 20.2$ and $r_0 = 23''$. The residual emission displayed a beautiful "grand-design" spiral structure. A strong rotation of the isophotes in the inner region of the galaxy was also apparent. There is essentially no bulge, and there are hints of such a structure only at radii of less than $3''$, we cannot deduce its profile due to the limited spatial resolution of our obbservations. However, a compact circumnuclear bar with a radius of about $7''$ is clearly visible, with spirals emerging from it ends, which are red, short, and turning *to meet* the more outer blue spiral arms (Fig. 2).

IC 499. A rotation of the isophotes is clearly visible at the center of the galaxy image (Fig. 2). The outer disk at $R > 55''$ is fairly weak and has a long radial scale, with $\mu_{V,0} = 21.2$ and $r_0 = 23''$. If it is neglected and an exponential profile is fitted at radii $20''-55''$, this yields an exponential disk with $\mu_{V,0} = 20.4$ and $r_0 = 17.4''$. After subtracting this model for the outer disk, this leaves an image indicating the presence of low-contrast, strongly wound spiral arms, although, in the outer part of the image, this may be discontinuous rings rather than arms, as is suggested in HYPERLEDA. The outer ring of IC 499 is distinguished by it blue color in the color map (Fig. 2). It is interesting that the very deep R surface-brightness profile for this galaxy extending to radii of more than $150''$ is interpreted in [19] using an exotic model: Type II (with a truncated brightness profile) in the inner region and Type III with a more shallow outer exponential segment in the outer regions. In fact, we were able to successfully fit the tabulated brightness profile from [19] using exponential segments *with the same scale*, $16.7''$, in the radius intervals $20''-40''$ and $80''-100''$; this scale coincides with the one we found for the inner disk. It is obvious that, in fact, the surface-brightness profile of the IC 499 disk has a single exponential scale of about $17''$, but a whole series of rings is present in the galaxy, whose brightness hinders fitting with a single exponential profile (Type I) in the full interval of distances from the center. After subtracting this disk from the initial image, it is possible to fit a circumnuclear disk, due to the very good seeing: $\mu_{V,0} = 18.1$ and $r_0 = 3''$. After subtracting this component, there remains an excellent bar with a modest thickening in the central region, which is apparently a classical bulge with Sersic index $n \approx 2$.

NGC 2300. We must first note the irregular shape of this galaxy: its isophotes more closely resemble an egg rather than a classical ellipse. The narrow end of the egg is located at the eastern side, in inner regions at $R < 40''$; farther out, the narrow end shifts toward the western side (Fig. 4). We believe that there are clear difficulties with the morphological classification of the galaxy in early catalogs, namely the atlas [20] and the Upsala General Catalog, which classify the galaxy as elliptical. In later photometric surveys, beginning with [8], and especially the relatively recent surveys [16, 19, 21], it is firmly demonstrated that the galaxy is an SA0 lenticular with an extended exponential disk having a single scale over the entire range of radii (Type I [19]). We measured the thickness of this disk using our new method [22], which is suitable for exponential stellar disks; it proved to be a completely standard lenticular-galaxy disk, $q = 0.4$. However, although all the photometric data indicate the presence of a bulge and extended stellar disk, the situation with the decompsing the galaxy into a disk and bulge is quite unclear. The exponential scales of the disk measured (very certainly!) in different studies are different, and clearly depend on the depth of the photometry and the interval of radii on which the surface brightness is fitted with an exponential profile. For example, using the least deep data in the V filter and radii to $R \approx 80''$, the scale $r_0 = 21''$, or 3 kpc, was obtained in [21]; our own fitting at radii of $80''-140''$, also in V, yielded the exponential scale $r_0 = 60''$, or 9 kpc, which, generally speaking, seems large for a normal disk galaxy. However, the most surprising result was obtained in [19]: an exponential profile with the scale $141.4''$, or 20.8 kpc, was fitted without any difficulty in the radius interval $R = 200''-530''$!

For comparison, Fig. 3 also shows the R-band surface-brightness profile measurements for NGC 2300 from [19] next to our own V measurements, together with the fitted exponential laws we found in [19]. For comparison, we also present in the right-hand panel our V exponential law, renormalized to the R filter assuming a uniform (see Fig. 4) color $V - R \approx 0.7$. This demonstrates that our new exponential cannot describe the central part of the NGC 2300 brightness profile from [19]. It is simply a mystery how it is possible to obtain such different surface brightnesses for such a uniform galaxy with a smooth color distribution as NGC 2300. Suspecting that the basis for this disagreement was that NGC 2300 was not a disk galaxy, we also fitted the surface-brightness profile with a de Vaucouleur law, which yielded $\mu_{V,e} = 19.9$ and $r_e = 14.9''$, or 2.2 kpc, with a mean scatter of the observational points about the model values of 0.07^m per square arcsec, which, generally speaking, appreciably exceeds the uncertainty in the azimuthally averaged profiles.

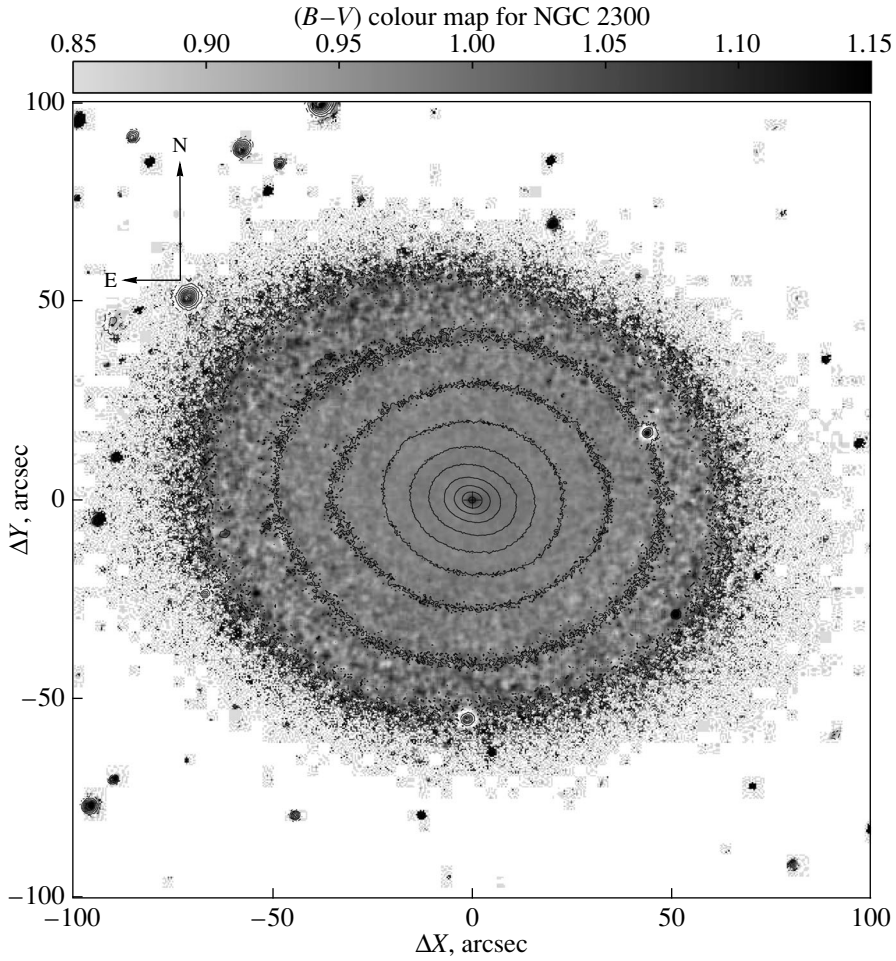

Fig. 4. $B-V$ color map for NGC 2300. On top of the color map given by gray gradations, the V isophots are also shown.

5. CONCLUSION

We have presented the results of a photometric study of five galaxies that are members of the "poor" galaxy group NGC 2300. These include three lenticular and two early-type spiral galaxies. We have constructed $B-V$ color maps, carried out an isophote analysis, and anayzed the surface-brightness profiles of these galaxies.

We wish to note here an interesting property of the NGC 2300 group: all the studied disk galaxies in the group have bars, suggesting that each of them is subject to tidal interactions, due to either other galactic members of the group or to intruders. Although the distances between the galaxies in this group are roughly the same as in the NGC 80 group, such a large number of galaxies with nested structures is not observed in the latter [23].

We noted a *reduced* percent of bars and an enhanced percent of ring structures in disk galaxies in the NGC 524 group [24]. The NGC 2300 group behaves completely differently from this. The first explanation that comes to mind is that we are dealing with two groups rather than one; the NGC 2300 and NGC 2276 subgroups are in the process of merging, and the disks of the member galaxies of both groups are subject to especially strong tidal interactions. Judging from its radial velocity, the galaxy UGC 3654 belongs to the latter of these subgroups, while IC 455 is obviously "bound" to NGC 2300. Both spiral galaxies are fairly far from the central galaxies in their groups, but their radial velocities suggest that they both belong to the overall NGC 2300 subgroup.

Several interesting papers have been written about interactions between the galaxies NGC 2300 and NGC 2276 and their groups. For example, the distribution of hot gas has been mapped using data from the ROSAT, and later the ASCA, X-ray satellites. The smoothed image in [9] shows that the center of the X-ray distribution does not coincide with either of the central galaxies of the group, and is shifted from NGC 2300 toward NGC 2276. However, the images of [25], where the superposition of several ROSAT exposures yielded an increased signal-to-noise, en-

abling less severe smoothing, show that NGC 2300 and NGC 2276 have individual X-ray halos. This is more clearly visible in the ASCA data [26]. Therefore, it is not ruled out that Makarov and Karachentsev [1] are right that these are two separate (according to their dynamics) groups. This would also explain discrepancies in estimates of the masses of the group: X-ray observations analyzed assuming the gas is in hydrostatic equilibrium yield $1.5 \times 10^{13}\ M_\odot$ [25], while the galaxy dynamics of [1] indicate a total mass for the two groups a factor of two lower.

ACKNOWLEDGMENTS

The data used in this study were obtained on the 6-m telescope of the Special Astrophysical Observatory of the Russian Academy of Sciences. Such observations are supported financially by the Ministry of Education and Science of the Russian Federation (agreement No. 14.619.21.0004, project identifier RFMEFI61914X0004). We thank Aleksei Moiseev for conducting the observations analyzed in this study. In our analysis, we used the Lyon–Meudon Extragalactic Database (LEDA), provided by the LEDA team at the Lyon Observatory of CRAL (France), and the NASA/IPAC extragalactic database (NED), managed by the Jet Propulsion Laboratory of the Calinfornia Institute of Technology under contract to NASA (USA). This work was supported by the Russian Science Foundation (project 14-22-00041).

REFERENCES

1. D. Makarov and I. Karachentsev, Mon. Not. R. Astron. Soc. **412**, 2498 (2011).
2. R. A. Pildis, J. N. Bregman, and A. E. Evrard, Astrophys. J. **443**, 514 (1995).
3. J. S. Mulchaey, D. S. Davis, R. F. Mushotzky, and D. Burstein, Astrophys. J. **456**, 80 (1996).
4. O. K. Silchenko and V. L. Afanasiev, Astron. Rep. **52**, 875 (2008).
5. J. P. Huchra and M. J. Geller, Astrophys. J. **257**, 423 (1982).
6. A. M. Garcia, Astron. Astrophys. Suppl. Ser. **100**, 47 (1993).
7. R. B. Tully, L. Rizzi, E. J. Shaya, H. M. Courtois, D. Makarov, and B. A. Jacobs, Astron. J. **138**, 323 (2009).
8. G. de Vaucouleurs, A. de Vaucouleurs, H. G. Corwin, Jr., R. J. Buta, G. Paturel, and P. Fouqué, *Third Reference Catalogue of Bright Galaxies,* Vol. 1: *Explanations and References* (Springer, New York, 1991).
9. J. S. Mulchaey, D. S. Davis, R. F. Mushotzky, and D. Burstein, Astrophys. J. **404**, L9 (1993).
10. H. C. Arp, Astrophys. J. Suppl. **14**, 1 (1966).
11. J. J. Condon, Astrophys. J. Suppl. **54**, 459 (1983).
12. V. L. Afanasiev and A. V. Moiseev, Astron. Lett. **31**, 194 (2005).
13. M. Michard and J. Marchal, Astron. Astrophys. Suppl. Ser. **105**, 481 (1994).
14. P. Goudfrooij, L. Hansen, H. E. Jorgensen, H. U. Norgaard-Nielsen, T. de Jong, and L. B. van den Hoek, Astron. Astrophys. Suppl. Ser. **104**, 179 (1994).
15. V. V. Vlasyuk, Astrofiz. Issled. **36**, 107 (1993).
16. E. Laurikainen, H. Salo, R. Buta, J. H. Knapen, and S. Comerón, Mon. Not. R. Astron. Soc. **405**, 1089 (2010).
17. J. L. Sérsic, *Atlas de Galaxies Australes* (Observat. Astron., Cordoba, 1969).
18. K. C. Freeman, Astrophys. J. **160**, 767 (1970).
19. L. Gutiérrez, P. Erwin, R. Aladro, and J. E. Beckman, Astron. J. **142**, id. 145 (2011).
20. A. Sandage and J. Bedke, *The Carnegie Atlas of Galaxies* (Carnegie Inst. of Washington Press, Washington, DC, 1994).
21. B. T. Dullo and A. W. Graham, Astrophys. J. **768**, id. 36 (2013).
22. E. M. Chudakova and O. K. Silchenko, Astron. Rep. **58**, 281 (2014).
23. M. A. Startseva, O. K. Silchenko, and A. V. Moiseev, Astron. Rep. **53**, 1101 (2009).
24. M. A. Il'ina and O. K. Silchenko, Astron. Rep. **56**, 578 (2012).
25. D. S. Davis, J. S. Mulchaey, R. F. Mushotzky, and D. Burstein, Astrophys. J. **460**, 601 (1996).
26. Y. Tawara, Y. Sakima, K. Yamashita, and R. Mushotzky, *Dark Matter*, Ed. by S. S. Holt and C. L. Bennett, AIP Conf. Proc. **336**, 268 (1995).

Translated by D. Gabuzda